

New false colour mapping for image fusion

Alexander Toet, & Walraven, J.

Copyright 1996 Society of Photo-Optical Instrumentation Engineers.

This paper was published in

Optical Engineering, 35(3), pp. 650-658

and is made available as an electronic reprint with permission of SPIE.

One print or electronic copy may be made for personal use only. Systematic or multiple reproduction, distribution to multiple locations via electronic or other means, duplication of any material in this paper for a fee or for commercial purposes, or modification of the content of the paper are prohibited.

New false color mapping for image fusion

Alexander Toet, MEMBER SPIE

Jan Walraven

TNO Human Factors Research Institute

Kampweg 5

3769-DE Soesterberg, The Netherlands

E-mail: toet@tm.tno.nl

Abstract. A pixel-based color-mapping algorithm is presented that produces a fused false color rendering of two gray-level images representing different sensor modalities. The resulting images have a higher information content than each of the original images and retain sensor-specific image information. The unique component of each image modality is enhanced in the resulting fused color image representation. First, the common component of the two original input images is determined. Second, the common component is subtracted from the original images to obtain the unique component of each image. Third, the unique component of each image modality is subtracted from the image of the other modality. This step serves to enhance the representation of sensor-specific details in the final fused result. Finally, a fused color image is produced by displaying the images resulting from the last step through, respectively, the red and green channels of a color display. The method is applied to fuse thermal and visual images. The results show that the color mapping enhances the visibility of certain details and preserves the specificity of the sensor information. The fused images also have a fairly natural appearance. The fusion scheme involves only operations on corresponding pixels. The resolution of a fused image is therefore directly related to the resolution of the input images. Before fusing, the contrast of the images can be enhanced and their noise can be reduced by standard image-processing techniques. The color mapping algorithm is computationally simple. This implies that the investigated approaches can eventually be applied in real time and that the hardware needed is not too complicated or too voluminous (an important consideration when it has to fit in an airplane, for instance). © 1996 Society of Photo-Optical Instrumentation Engineers.

Subject terms: sensor fusion; low-level image fusion; multisensor fusion; color mapping; false color.

Paper SF-011 received July 11, 1995; revised manuscript received Aug. 29, 1995; accepted for publication Oct. 3, 1995.

1 Introduction

1.1 The Goal of Multispectral Image Fusion

Visual information display is an important component of most visually guided systems. In many modern applications, synthetic displays have replaced direct viewing. One advantage of this modern technology is the ability to provide more information than that available to the unaided eye.

In recent years, new image sensors have been introduced that provide a greater range of information to users, and that may permit human operators to perform visually guided tasks even in adverse weather and lighting conditions. The different sensors provide different information about the scene and are effective in different environmental conditions. For example, thermal sensors enable operations in the dark, whereas millimeter wavelength radiation is more effective in fog. A system that may help a pilot to fly in conditions with reduced visibility may therefore be achieved by combining the outputs of thermal and passive millimeter wave cameras, preferably supported by data-

bases of the terrain. (Images rendered from a database can compensate for the low spatial resolution of the sensor images.)

Image fusion can be defined as the process of combining two or more source images into a single composite image with extended information content. Image fusion is particularly useful for reducing the workload of human operators. Without fusion, an operator must move his eyes between displays or switch between sensors to observe one sensor modality at a time. It may be difficult for him to recognize relationships among patterns, since the image of the same object can appear quite different in different modalities. Even determining the correspondence of patterns in different images may be nearly impossible for a human. The integration of information across multiple human operators is nearly impossible. Fusion may provide the means for an observer to perceive all the available visual information at a single glance, in correct registration.

The above mentioned considerations have resulted in an increased interest in fusion methods, as is reflected in a steadily growing number of publications on this topic.¹⁻¹⁰

1.2 Previous Approaches to Multispectral Image Fusion

Fusion of sensor information can take place at different levels of signal abstraction; e.g., at the signal, pixel feature and symbol level.¹¹ This study specifically addresses the problem of pixel-level fusion. Pixel-level fusion serves to increase the useful information content of an image so that performance in perceptual tasks such as segmentation and feature detection can be improved.

No information should be lost in the image fusion process. Not only the structure, but also the origin of the details from the different image modalities should therefore be clearly represented in the fused image. Preferably the resulting image should also have a natural appearance so that it can be readily interpreted.

Most previous image fusion schemes produce gray-level images as output.¹⁻¹⁰ Although the composite images that are produced by these schemes present a more detailed representation of the depicted scene than either of the input images alone, there is no way to tell from which modality the details in the final result originate. Knowledge of the origin of certain details may provide essential information about the object of interest (e.g., whether the engine of a vehicle is still running). Detection, recognition and search, and also navigation tasks may benefit considerably from a representation of the fused image that clearly displays the type of information that the local image details represent.

1.3 Multispectral Image Enhancement

Enhancement procedures are often performed on the individual bands of multispectral images to accentuate certain features to assist in subsequent human interpretation or machine analysis.¹² These procedures include individual image band enhancement techniques such as contrast stretching, noise cleaning and edge crispening.

Other enhancement methods involve the joint processing of multispectral bands. Images are usually spatially correlated because of regularities in the depicted scene. The different bands of multispectral images are generally correlated because the bands represent (different aspects of) the same underlying physical scene. The joint processing of multispectral bands serves to enhance details that are unique to a certain band by reducing the relative contribution of the common component of the different bands.^{12,13} For instance, the pairwise subtraction of multispectral bands accentuates reflectivity variations between them and removes unknown common bias components. Another effective means of multispectral image enhancement is the elimination of variations in illumination by the formation of ratios of the image bands.^{14,15}

The spatial and intraband correlation of image signals can simultaneously be reduced through a combined decorrelation and redundancy reduction operator.¹⁶ This operator is modeled after the spatiochromatic antagonistic organization of the receptive fields in the visual system. It performs spatial decorrelation through linear predictive coding and intraband (color) decorrelation through transform coding.

Waxman et al.¹⁷ recently presented a color mapping scheme that employs a spatiochromatic antagonistic kernel. The kernel is convolved with registered thermal and intensified visual images. The resulting spatially and spectrally contrast-enhanced (redundancy reduced) images are then

displayed through the red and green channels of a color display. Color renderings of night scenes thus produced have a natural appearance. However, only convolution kernels of a single spatial scale are used. As a result, the resolution of the fused images is limited by the spatial scale parameter of the kernel.

Ultimately the performance of a fusion process must be measured as the degree to which it enhances a viewer's ability to perform certain tasks such as recognition or detection.

The fusion of images may have different perceptual effects.¹⁸ A fused image may be perceptually (a) advantageous, i.e., it may provide a perceptually more complete or useful representation; (b) disadvantageous, i.e., details in one image may hide or mask details in the other image so that the combined image is less detailed or useful than either of the original images; and (c) impossible, because it does not represent a visible physical situation or process. The particular outcome of the fusion process probably depends on the degree of local spatial correlation between the individual images.¹⁹

It has been shown that degraded (blocked and low-pass frequency filtered) images are discriminated better when they are fused in pairs than when they are presented separately.¹⁸ Color-coded information can be acquired even more quickly and with greater accuracy than achromatic information.²⁰ Also, fewer fixations are required to locate color-coded targets.²¹ Walraven and Lucassen²² used a false color* mapping to fuse the output of two image intensifier tubes with different spectral sensitivities. In an evaluation study of human observer performance with this representation, they found that, due to the false color information, speed and accuracy for target detection are boosted by 30 and 60% respectively.²³

1.4 A New Enhanced Color Mapping

The method presented here produces a fused false color rendering of two gray-level images representing different sensor modalities. First, the common component of the two original input images is determined. Second, the common component is subtracted from the original images to obtain the unique component of each image. Third, the unique component of each image modality is subtracted from the image of the other modality. This step is similar to the aforementioned color-opponency found in biological color vision. It serves to enhance the representation of sensor-specific details in the final fused result. Finally, a fused color image is produced by displaying the images resulting from step 3 through, respectively, the red and green channels of a color display. The method is used to fuse thermal and visual images. The results show that the color mapping

* False color is a point-by-point mapping of a set of multispectral image planes of a scene to a color space defined by display tristimulus values that are functions of the original image pixel values (e.g., Refs. 24 and 25). False color can be used (a) to match the color sensitivity of the human eye, (b) to segment certain details from their background so that they can be perceived more easily, and (c) to produce a natural color representation of a set of multispectral images of a scene. Note that the multispectral images may be obtained from sensors with a wavelength response outside the visible wavelength range, for example, infrared or ultraviolet.



(a)



(b)

Fig. 1 (a) Original intensified visual (TV) and (b) thermal (IR) aerial

enhances the visibility of certain details and preserves the specificity of the sensor information. The fused images also have a fairly natural appearance.

The fusion scheme involves operations only on corresponding pixels. The resolution of a fused image is therefore directly related to the resolution of the input images. Before fusing, the contrast of the images can be enhanced and their noise can be reduced by standard image-processing techniques.

The color mapping algorithm is computationally simple. This implies that the investigated approaches can eventually be applied in real time and that the hardware needed is not too complicated or too voluminous (an important consideration when it has to fit in an airplane).

2 Methods and Results

The methods presented in this section will be illustrated on two sets of registered visual and thermal images. Figure 1(a) is an intensified video image (TV), representing an aerial view of a terrain with vegetation, buildings and roads. The image intensifier has a spectral sensitivity range



(a)



(b)

Fig. 2 (a) Original video (TV) and (b) thermal (IR) images of a

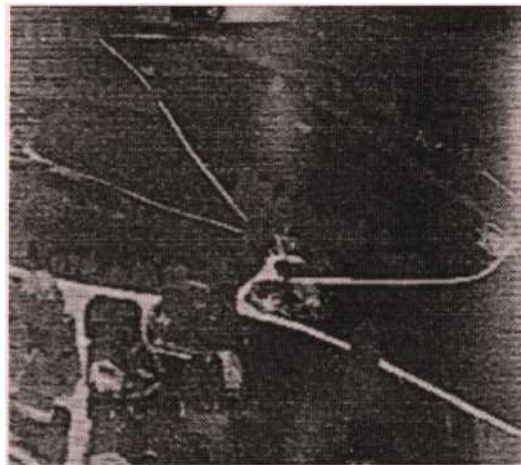
of 0.4 to 0.9 μm . Figure 1(b) is the corresponding thermal image (IR), with the same dimensions as Fig. 1(a). The thermal camera has a spectral sensitivity range of 8 to 12 μm . The images were recorded at night from a helicopter.

Figure 2 shows the original (a) video and (b) thermal image of a tank. The video image was taken with a standard CCD camera. The thermal image was made with a Philips Usfa UA8012 FLIR camera, also with a spectral sensitivity range of 8 to 12 μm .

All images used in this study consist of 256X256 pixels with 8 bits of gray-scale resolution. They are first warped so that corresponding points of the scene are mapped onto pixels with the same coordinates. In Fig. 1(b) the effect of this warping can be seen in the upper and lower parts of the image because the angular size of the vertical extent of the field of view of the FLIR camera is less than the corresponding extent of the video camera. The registered images are then normalized in contrast. This can, for instance, be done through adaptive histogram equalization (e.g., Ref. 25). However, any other method that locally enhances and



(a)

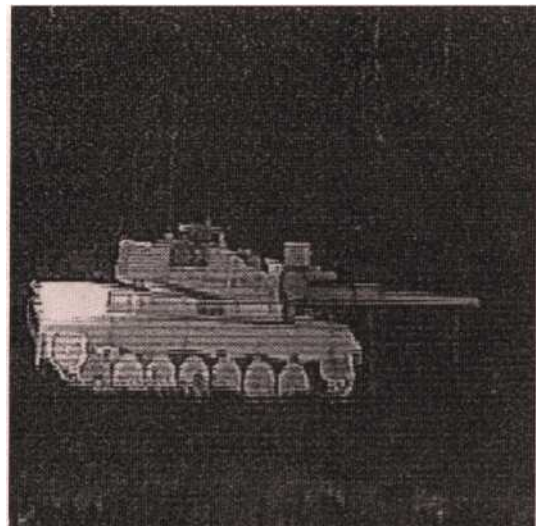


(b)

Fig. 3 The images of Fig. 1 after contrast enhancement.



(a)



(b)

Fig. 4 The images of Fig. 2 after contrast enhancement.

normalizes image contrast can also be used. The histogram-equalized versions of Figs. 1 and 2 are shown in Figs. 3 and 4.

The next step is the computation of the common component of the images. This is simply implemented as a local minimum operator. The common component of two images $A(i,j)$ and $B(i,j)$ is therefore given by

$$A \cap B(i,j) = \text{Min}\{A(i,j), B(i,j)\}, \quad (1)$$

where A and B represent sampled 2-D luminance functions or digital images, and i,j represent the indices of an element of the sampling grid (the pixel coordinates; $\{i,j\} \in [1,256]$, $\{A,B\} \in [0,255]$). The common component of the images from Figs. 3 and 4 is shown in Figs. 5(a) and 5(b).

The unique or characteristic component of each image remains after subtraction of the common component. The characteristic components A^* and B^* of two registered images $A(i,j)$ and $B(i,j)$ are defined as

$$A^* = A - A \cap B, \quad \text{and} \quad (2)$$

$$B^* = B - A \cap B. \quad (3)$$

The characteristic components of the images from Figs. 3 and 4 are shown in Figs. 6 and 7. These images represent the details that are unique to the corresponding image modalities.

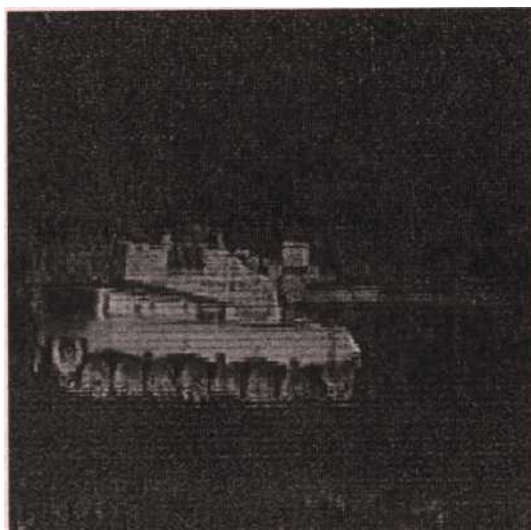
The characteristic components A^* and B^* can be emphasized in the fused image C by subtracting them from A and B before fusion:

$$C = (A - B^*) \bowtie (B - A^*), \quad (4)$$

where \bowtie represents the fusion operator, which represents any operation that effectively combines information from two input images into a single output image. The subtraction operation has been arbitrarily chosen. Any operation that reduces the dynamic range of one image at locations where the characteristic component of the other image has an appreciable value can in principle be used.



(a)



(b)

Fig. 5 The common component ($TV \cap IR$) of the images of (a) Fig. 3 and (b) Fig. 4.

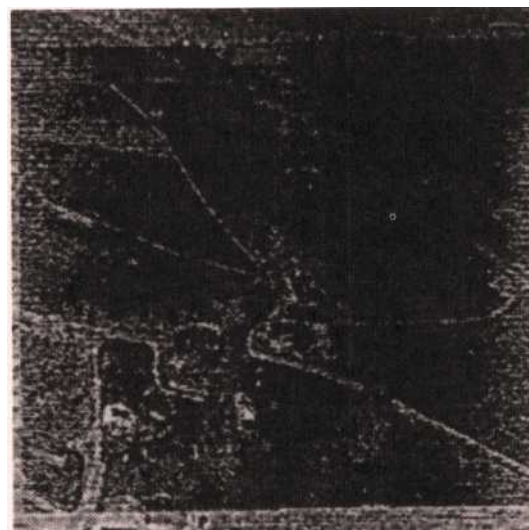
The result of this operation is illustrated by Figs. 8 and 9. Figures 8(a) and 9(a) show the signal $TV - IR^*$, corresponding to the difference between, respectively, (a) Figs. 3(a) and 6(b) and (b) Figs. 4(a) and 7(b). Similarly, Figs. 8(b) and 9(b) represent the signal $IR - TV^*$, which corresponds to the difference between, respectively, (a) Figs. 3(b) and 6(a), and (b) Figs. 4(b) and 7(a). This operation reduces the local contrast in the image of a certain modality when there is a detail with an appreciable contrast at the same location in the corresponding image of the other modality.

The resulting images can then be combined into a composite false color image by representing the processed thermal image through the red channel and the processed video image through the green channel of a red-green-blue (RGB) display:

$$\begin{pmatrix} R \\ G \\ B \end{pmatrix} = \begin{pmatrix} IR - TV^* \\ TV - IR^* \\ 0 \end{pmatrix}. \quad (5)$$



(a)

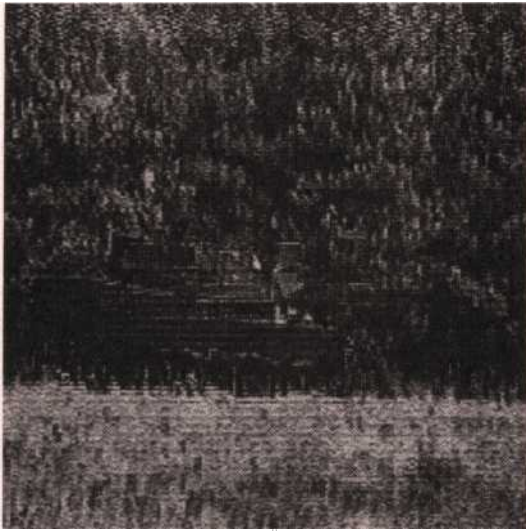


(b)

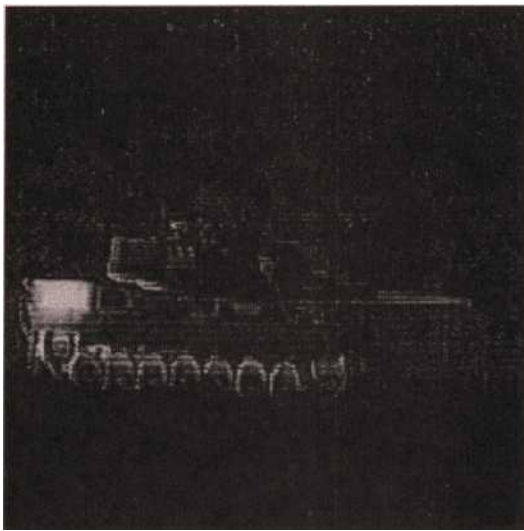
Fig. 6 The characteristic component of (a) the video image of Fig. 3(a) ($TV^* = TV - TV \cap IR$) and (b) the thermal image of Fig. 3(b) ($IR^* = IR - TV \cap IR$).

Figure 10 shows the result of this operation. Figure 10(a) is obtained by assigning Fig. 8(b) to the red channel and Fig. 8(a) to the green channel of an RGB display. Similarly, Fig. 10(b) is obtained by assigning Fig. 9(b) to the red channel and Fig. 9(a) to the green channel. Some details are more easily seen and can be better recognized in the fused images than in the individual input images.

The between-modality subtraction of characteristic details in the color rendering of the fused result. Because the color of details in the fused images is saturated, they can be more easily discriminated. For example, in Fig. 10(a) all windows of the leftmost house in the lower part of the scene are clearly visible. The walls are rendered in red, the upper windows in green and the lower windows in yellow. The walls are colored red because they are represented with a high positive contrast in the thermal image because they are warmer than their local background, whereas they are rep-



(a)

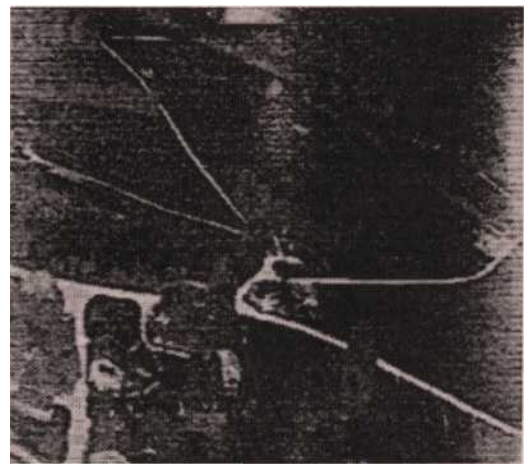


(b)

Fig. 7 The characteristic component of (a) the video image of Fig. 4(a) (TV^*) and (b) the thermal image of Fig. 4(b) (TV^*).



(a)



(b)

Fig. 8 The difference of (a) the video image of Fig. 3(a) and Fig. 6(b) [the characteristic component of the thermal image of Fig. 3(b): $TV-IR^*$], and (b) the thermal image of Fig. 3(b) and Fig. 6(a) [the characteristic component of the video image of Fig. 3(a): $IR-TV^*$].

resented with a negative contrast in the video image because they reflect less light than their surroundings. The lower windows are not at all visible in the thermal image because they had the same temperature as the walls.

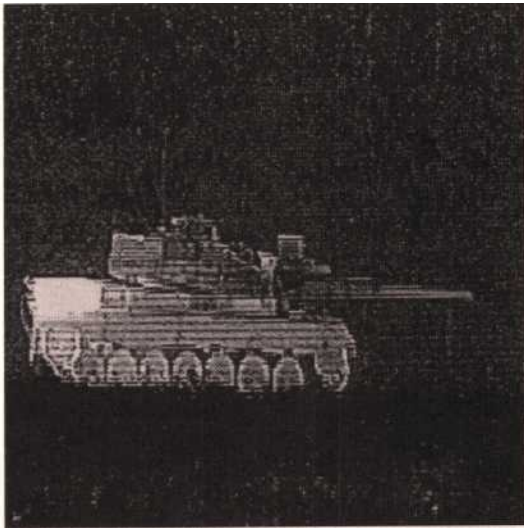
The image intensity at the location of the lower windows is almost the same for both sensor modalities. As a result they are rendered in yellow in the fused image. The upper windows have a high positive contrast in the video image and a large negative contrast (low intensity) in the corresponding thermal image. The contribution of the video image therefore dominates at this location and the windows are rendered in green in the fused color image. The narrow road running from the center of the image to the left edge of the image has a high positive contrast in the thermal image, but is not visible in the video image. However, the mean intensity of the video image is relatively high at the location of this road. The road is therefore rendered in orange in the fused image. The roof of the house on the lower right has a high positive contrast in the thermal image and

a large negative contrast in the video image. It is colored red in the fused image. Summarizing, houses, vegetation and roads can be seen and recognized easier in the fused image than in either of the individual images. Moreover, the origin of the details in the fused image can easily be deduced from their color. In the case of video and thermal images, this means that the information about the temperature and reflectance of details is still available.

In Fig. 10(b) the back of the tank is clearly visible. This part is represented with a large positive contrast in the thermal image. In the video image, the same part is depicted with a small negative contrast and has almost the same luminance as the shadows in the background. As a result, the overall shape of the tank is not easily seen in the video image. In the fused image this shape is not only clearly delineated, but also colored red, which clearly indicates that this part has a high positive thermal contrast (a relatively warm part). The same holds for the front part of the barrel, which is barely visible in the video image, but returns



(a)



(b)

Fig. 9 The difference of (a) the video image of Fig. 4(a) and Fig. 7(b) [the characteristic component of the thermal image of Fig. 4(b): $TV - IR^*$], and (b) the thermal image of Fig. 4(b) and Fig. 7(a) [the characteristic component of the video image of Fig. 4(a): $IR - TV^*$].



(a)



(b)

Fig. 10 Fusion of (a) Figs. 8(a) and 8(b), and (b) Figs. 9(a) and 9(b) by representing the processed thermal images through the red channel and the processed video images through the green channel of an RGB display: $(R,G,B) = (IR - TV^*, TV - IR^*, 0)$.

clearly visible and colored in red in the fused image because this relatively warm part is represented with a high positive contrast in the corresponding thermal image.

The characteristic components of the individual images can be further underscored by assigning their difference to the blue channel of the RGB display:

$$\begin{pmatrix} R \\ G \\ B \end{pmatrix} = \begin{pmatrix} IR - TV^* \\ TV - IR^* \\ TV^* - IR^* \end{pmatrix}. \quad (6)$$

Figures 11(a) and 11(b) show the color rendition of the fused image when the difference between the images in Figs. 6 and 7 is assigned to the blue channel, and the red and green channels contain the same information as in Fig. 10. These examples show that the enhancement of the modality-specific details produces an image with more

color variation, which makes it intuitively easier to interpret. For instance, in the aerial reconnaissance image [Fig. 11(a)] the sky appears blue, the vegetation green and the walls red. This makes the scene look natural. Note that the input images were gray-scale images, recorded at night, while the fused image looks like a full-color image taken during daytime. The tank [Fig. 11(b)] also has some color contrast with its local background, and density variations in the grass in the foreground become visible: empty spots are depicted bluish because they have a lower intensity (reflectivity) in the video image.

As a comparison, Fig. 12 shows the gray-scale representation of the luminance component of Fig. 11. This image is comparable to the result of previously developed gray-scale image fusion algorithms. The luminance of each pixel is computed as a weighted mean of the corresponding images in the R, G and B components of Fig. 11:



(a)



(b)

Fig. 11 Figure 10, when the differences between the thermal and video images have been emphasized by representing the difference between respectively (a) Figs. 6(a) and 6(b), and (b) Figs. 7(a) and 7(b) through the blue channel of an RGB display: $(R,G,B)=(IR-TV^*, TV-IR^*, TV^*-IR^*)$.

$$L=0.30R+0.59G+0.11B, \tag{7}$$

where L denotes the luminance of the resulting gray-level image, and the coefficients represent the relative contribution of each color channel of a standard NTSC monitor to the perceived luminance.²⁶ This corresponds to a weighted average of the thermal image, the processed (enhanced) video image and the difference of the unique components of both aforementioned images.

A comparison of Figs. 11 and 12 shows that objects like houses, roads and vehicles can be more easily distinguished from their local background (segmented) in the color images than in the gray-scale images. This is because the color mapping gives these objects a color contrast with respect to their local background.



(a)



(b)

Fig. 12 Gray-level representation of Fig. 11.

3 Discussion

A new pixel-based color mapping to fuse thermal and visual images has been developed. The resulting color rendering enhances the visibility of certain details and preserves the specificity of the sensor information. The fused images also have a fairly natural appearance. Consequently, visual target detection and recognition performance may be expected to benefit in terms of both speed and precision.

The algorithm operates only on corresponding pixel values. As a result, it does not degrade the resolution of the final result. Standard image processing techniques can be used to enhance image contrast or extract image features prior to the fusion process. The fusion scheme involves only simple operations. The method can therefore probably be applied in real time and with relatively simple hardware.

The practical value of the method will be tested through a series of observer experiments in realistic military see-

narios. Detection and recognition performance with fused imagery will be compared with the performance that can be obtained with the original (unfused) imagery.

Acknowledgment

The aerial images used in this study are the property of Daimler-Benz AG/Eurocopter Deutschland GmbH.

References

1. P. Ajijmarangsee and T. L. Huntsberger, "Neural network model for fusion of visible and infrared sensor outputs," in *Sensor Fusion Spatial Reasoning and Scene Interpretation, Proc. SPIE, 1003*, 153-160 (1988).
2. P. J. Burt, "A gradient pyramid basis for pattern-selective image fusion," in *Proc. SID Int. Symposium 1992. Soc. for Information Display*, Playa de Rey, CA, pp. 467-470 (1992).
3. P. J. Burt and R. J. Kolczynski, "Enhanced image capture through fusion," in *Proc. Fourth Int. Conf. on Comp. Vision*, pp. 173-182, IEEE Comp. Soc. Press, Washington, DC (1993).
4. T. Fechner and G. Godlewski, "Optimal fusion of TV and infrared images using artificial neural networks," *Proc. SPIE 2492*, 919-925 (1995).
5. H. Li, B. S. Manjunath, and S. K. Mitra, "Multisensor image fusion using the wavelet transform," *Graphical Models Image Proc.* 57, 235-245 (1995).
6. A. Toet, "Image fusion by a ratio of low-pass pyramid," *Pattern Recog. Lett.* 9, 245-253 (1989).
7. A. Toet, "Hierarchical image fusion," *Machine Vision Appl.* 3, 1-11 (1990).
8. A. Toet, "Adaptive multi-scale contrast enhancement through non-linear pyramid recombination," *Pattern Recog. Lett.* 11, 735-742 (1990).
9. A. Toet, "Multi-scale contrast enhancement with applications to image fusion," *Opt. Eng.* 31, 1026-1031 (1992).
10. A. Toet, L. J. van Ruyven, and J. M. Valetton, "Merging thermal and visual images by a contrast pyramid," *Opt. Eng.* 28, 789-792 (1989).
11. R. Luo and M. Kay, "Data fusion and sensor integration: state of the art in the 1990s," in *Data Fusion in Robotics and Machine Intelligence*, M. Abidi and R. Gonzalez, Eds., pp. 7-136, Academic Press, San Diego (1992).
12. J. A. Richards, *Remote Sensing Digital Image Analysis*, Springer-Verlag, Berlin (1986).
13. V. D. Vaughn and T. S. Wilkinson, "System considerations for multi-spectral image compression designs," *IEEE Signal Proc. Mag.* 12, 19-31 (1995).
14. D. J. Granrath, "The role of human visual models in image processing," *Proc. IEEE* 69, 552-561 (1981).
15. J. F. Boulter, "Image enhancement by spectral ratioing," CRDV Report 4170/80, Research and Development Branch, Dept. of Defence, Quebec, Canada (1980).
16. J. B. Derrico and G. Buchsbaum, "A computational model of spatio-chromatic image coding in early vision," *J. Visual Commun. Image Representation* 2, 31-38 (1991).
17. A. M. Waxman, D. A. Fay, A. Gove, M. Seibert, J. P. Racamoto, J. E. Carrick, and E. D. Savoye, "Color night vision: fusion of intensified visible and thermal IR imagery," in *Synthetic Vision for Vehicle Guidance and Control, Proc. SPIE 2463*, 58-68 (1995).
18. W. R. Uttal, T. Baruch, and L. Allen, "Dichoptic and physical information combination: a comparison," *Perception* 24, 351-362 (1995).
19. T. Caelli and J. Yuzyk, "What is perceived when two images are combined?" *Perception* 14, 41-48 (1985).
20. R. E. Christ, "Review and analysis of colour coding research for visual displays," *Human Factors* 17, 542-570 (1975).
21. P. K. Hughes and D. J. Creed, "Eye movement behaviour viewing colour-coded and monochrome avionic displays," *Ergonomics* 37, 1871-1884 (1994).
22. J. Walraven and M. P. Lucassen, "Optimization of color rendering of a false color image intensifier" (in Dutch), Memo IZF 1992-M9 (1992).
23. J. Walraven and M. P. Lucassen, "Evaluation of visual performance of a false color image intensifier" (in Dutch), Report IZF 1994 C-02 (1994).
24. W. Fink, "Image coloration as an interpretation aid," *Proc. SPIE* 74, 209-215 (1976).
25. W. K. Pratt, *Digital Image Processing*, Wiley, New York (1991).
26. W. Niblack, *An Introduction to Digital Image Processing*. Prentice-Hall, Englewood Cliffs, NJ (1986).
27. O. D. Faugeras, Digital color image processing within the framework of a human visual model. *IEEE Trans. Acoustics, Speech Signal Proc.* 27, 380-393 (1979).
28. E. H. Land, The retinex theory of color vision. *Scientific American* 237, pp. 108-128 (1977).
29. J. Serra, Image analysis and mathematical morphology. Vol. 2: Theoretical advances. Academic Press, London, New York (ed., 1988).
30. A. Toet, Image fusion through multiresolution contrast decomposition. TNO-report IZF 1989-19 (1989b).
31. A. Toet, Multi-scale contrast enhancement with applications to image fusion. TNO-report IZF 1990 A-9 (1990c).
32. A. Toet, Multi-scale color image enhancement. *Pattern Recog. Lett.* 13, 167-174 (1992b).
33. A. Toet, Multi-scale image fusion, in *Proc. SID Int. Symposium 1992. Soc. for Information Display*, Playa de Rey, CA, pp. 471-474 (1992c).



Alexander Toet received his PhD in physics from the University of Utrecht in the Netherlands in 1987. He has published more than 40 papers on spatial vision and image processing. His current research interests are image fusion, mathematical morphology, the development of computational models for human visual search, and the quantification of target conspicuity.



Jan Walraven graduated from the University of Leiden in 1965 and then joined the TNO Institute for Perception in Soesterberg. Ever since he has worked on both basic and applied research projects, (co)-authoring more than 130 reports and publications, including chapters in text books. In 1981 he received his PhD in biophysics from the University of Utrecht, for his work on signal processing in color vision. He has been secretary of the International Color Association (AIC), is associate editor of the journal *Color Research & Application*, and is a member of the CIE Technical Committee TC 27, which is involved in evaluating color fidelity in electronic color reproduction. At present he is involved in developing a color deficiency simulator for use in an expert system that enables color-blind display users (8% of the male population) to have the color tables adjusted to their specific needs.